Chemical Accelerator Studies of Isotope Effects on Collision Dynamics of Ion–Molecule Reactions: Elaboration of a Model for Direct Reactions

P. M. HIERL,* Z. HERMAN,† AND R. WOLFGANG‡
Department of Chemistry, University of Colorado, Boulder, Colorado 80302
(Received 22 January 1970)

Crossed-beam studies on isotopic variants of the reaction $Ar^+ + H_2 \rightarrow ArH^+$ are reported. Both velocity and angular distributions of the ionic product as a function of initial translational energy, down to 0.1 eV (center of mass), have been measured. At lowest energies there is a gain in the translational energy of the products over that of the reactants, but at higher energies there is increasing conversion of kinetic into internal energy. While this represents the most probable course of the reaction there is a fairly wide distribution about the median values. Results confirm that this reaction is predominantly direct at all energies and provide no evidence for intermediate persistent complex formation. They are also consistent with a model for direct reactions previously proposed. The data on reaction with HD permit further development of this mechanism. The reactants are mutually accelerated by their long-range attractive potential until hydrogen atom transfer occurs. The liberated H (or D) atom is reflected from the ArD^+ (ArH^+) and the products separate, being decelerated in the process by the attractive potential acting between them. This "polarization–reflection" model yields a reasonable value for the radius at which transfer occurs, and it accounts quantitatively for the magnitudes of, and isotopic effects on, the median product velocities. It also predicts the significant back scattering observed at very low as well as very high energies. With appropriate modification for the attractive potentials involved the model can provide a simple representation of direct reactions in general.

Simple ion and atom transfer reactions are among the most common in chemical kinetics. Because of this and their apparent simplicity, considerable attention has recently been devoted to the detailed dynamics of such processes. Extensive studies, using molecular beam methods, have been made in alkali-atom–halide reactions at thermal energies. Simultaneously, ion–molecule reaction of the types

$$N_2^+ + D_2 \rightarrow N_2D^+ + D, \quad (1)$$

$$Ar^+ + D_2 \rightarrow ArD^+ + D, \quad (2)$$

have been investigated using accelerated ion beams in devices known as "chemical accelerators."

Henglein and collaborators[1] discovered some years ago that reactions such as (1) and (2), when occurring at high energies (greater than 25 eV lab) could be well described by what has become known as the spectator stripping model. The essential feature of this model is that the entity which has lost the transferred atom is not "aware" of its loss and proceeds with unchanged velocity. This model, though most fruitful, is naturally a first approximation to reality. In the high and extremely high energy range significant deviations, largely due to severe restraints imposed by momentum and energy conservation in very fast collisions, have been found by Henglein,[2] by Bailey,[3] and by Mahan.[4]

While results on high-energy chemical reaction ballistics can yield valuable data on the strong repulsive-core potentials, experiments at medium and low energies can better provide information on the weaker attractive forces which control chemical reaction. Development of the crossed-beam chemical accelerator EVA has permitted such downward extension of the accessible energy range to the near thermal region. Initial data on product velocity and angular distributions for reactions such as (1) and (2) were thus obtained[5] over a wide range of energies and immediately led to two important findings. First, it was found that such transfer processes did not, as had previously been supposed, necessarily involve a long-lived intermediate at low energies. Second, the mechanism, though remaining direct in the sense of not going through a persistent complex, deviated progressively from spectator stripping as the energy declined. These findings were subsequently confirmed by Fink[6] and by Henglein and collaborators.[7]

The spectator-stripping model, in effect, assumes that there are no forces acting between either the reactant or the product particles. We proposed[5] the replacement of this model by one more widely applicable to direct reactions, i.e., one which takes into account known attractive potentials.

This latter model states that as the reactants approach one another, they experience a long-range attractive force which accelerates them towards each other, so that by the time they have reached their distance of closest approach their relative velocity is greater than it had been at infinite separation. It is assumed that at this distance of closest approach, the short-range chemical forces become operative and effect the transfer in a direct manner. The products then recede from one another, being somewhat decelerated by the attractive potential existing between them. The net effect will generally be that the products have a higher relative velocity than expected from spectator stripping, although this need not always be the case.

Reactions between ions and polarizable molecules present a favorable test for this model since the ion-induced dipole potential which is presumably involved

is moderately strong (of the order of 1 eV). Our previously published data[5,8] on Reactions (1) and (2) demonstrated the ability of the model to predict successfully the peak value of the product velocity and the partition of product energy between internal and translational modes. It further provided information on the mean distance of closest approach.

As was recognized in its original formulation, this model, although quite successful, is necessarily deficient in not explicitly considering the effect of repulsive forces. These repulsive forces will manifest themselves in the change of velocity and kinetic energy of the particle being freed as its partner is being captured. Unfortunately, these short-range forces are not nearly as well understood as are the longer-range attractive potentials. Furthermore, they are liable to vary considerably from system to system. It is nevertheless useful to attempt to take them into account in a crude but general manner.

Two possible elaborations of the model may therefore be proposed:

(I) The repulsive forces are assumed to have no effect on the particle being freed [D in Reactions (1) and (2)], so that its trajectory is governed purely by attractive forces. We call this the "polarization-stripping" model.[9] Such a model might apply if the bond in the approaching molecule [D_2 in Reactions (1) and (2)] was so weakened just prior to reaching the turning point that the particles were essentially travelling independently. The stripping hypothesis suggests that the speed of the freed neutral particle is modified only by the attractive forces between the approaching reactants and receding products and will, therefore, remain unchanged during the actual transfer.

(II) Alternatively, it may be more realistic to consider that during the transfer the particle being freed is reflected from a repulsive core potential. This means that its velocity may change, the extent of the change being dependent on relative masses and angle of impact on the reacting surface. The elasticity of the reflecting surface is also a factor and "elastic," "superelastic," and "subelastic" reflections may be defined and distinguished. Such a model would be a more appropriate description if the incoming molecule remains strongly bound until the time of transfer. Figure 8 in Ref. 5(b) illustrates and implies this variation of the basic mechanism.

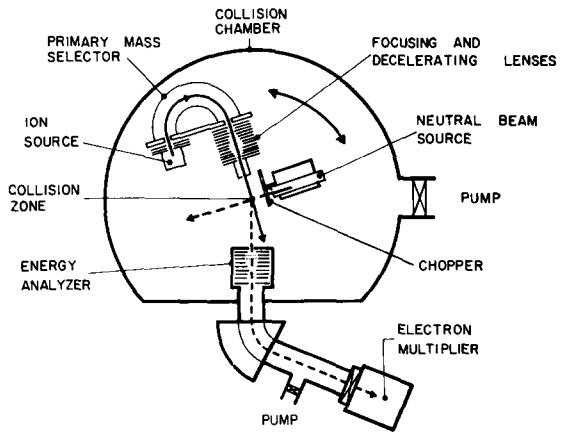

FIG. 1. Schematic representation of EVA as modified by addition of the primary mass selector.

Earlier data[5] on Reactions (1) and (2) were consistent with the speed of D remaining unchanged at the moment of transfer. As will be shown later in this article, the fact that the captured and the freed particle have similar masses makes these results consistent with either model. We were thus unable to distinguish between the polarization-stripping and the polarization-elastic-reflection mechanisms, although if the latter is correct, the implication is that the reflection is elastic within experimental error.

To provide the further necessary information for the elaboration of this model we have studied the reactions,

$$Ar^+ + HD \rightarrow ArH^+ + D \quad (3a)$$

$$\rightarrow ArD^+ + H. \quad (3b)$$

The dynamical isotope effects on both velocity and angular distributions of the ionic products were measured. If the polarization-stripping model is the better approximation, then the velocities of the freed D or H atoms should be the same, even at low energies. If polarization elastic reflection is more appropriate, then in the limit of zero initial energy, the kinetic energies of the freed D or H atoms should be similar and their velocities differ accordingly.

For purposes of comparison, data was also obtained for the further isotopic variant,

$$Ar^+ + H_2 \rightarrow ArH^+ + H. \quad (4)$$

A more detailed development of both models is presented. It appears that the polarization-elastic-reflection mechanism provides a representation of our experimental data which is sufficient within experimental accuracy.

EXPERIMENTAL

EVA

The apparatus EVA (Evatron), shown schematically in Fig. 1, is a crossed-beam instrument for the study of ion–molecule reactions over the energy range 0.1–25 eV(cm). Ions, formed by electron impact, pass through a 180° mass spectrometer and a collimating system of decelerating electrostatic lenses into the collision zone, where the ion beam is intersected at 90° by a modulated molecular beam of thermal energy[10] at 55°C. Ions from

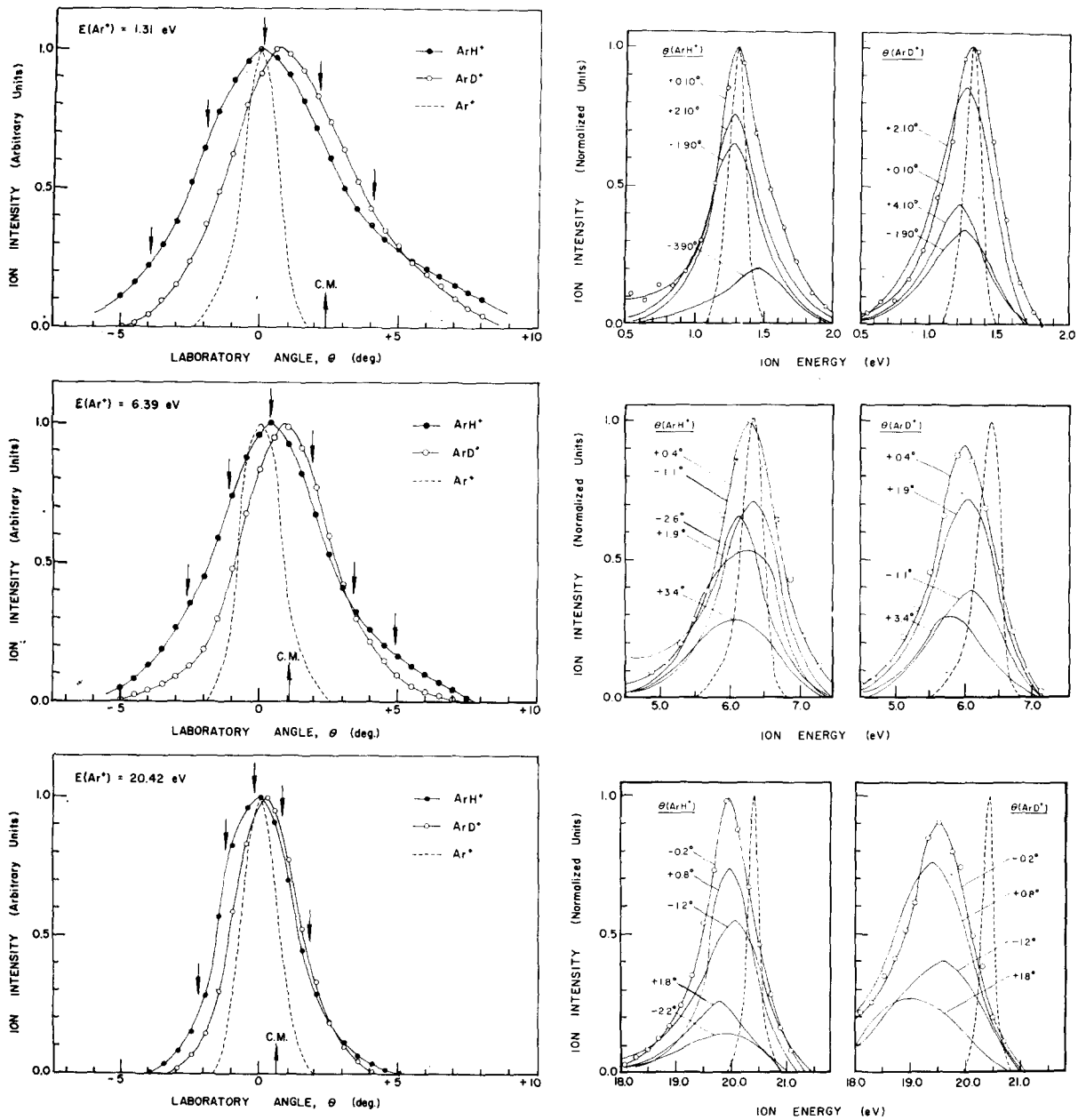

FIG. 2. Data on $Ar^+ + HD = ArH^+(ArD^+) + D(H)$ reaction at three lab energies of Ar^+. Angular plots (on the left) are normalized to unity for both reactant and product ions. The laboratory angle of the center-of-mass motion is indicated (c.m.). On the right are shown product energy distributions taken at the angles indicated by arrows. Areas under the energy spectra correspond to total relative intensity at the given angle. Dotted lines show energy spectra of primary Ar^+ beams.

the collision zone pass through a detection slit (0.2 mm wide by 1.0 mm high), a stopping-potential-energy analyzer, a 60° sector mass spectrometer, and are detected by an electron multiplier. Since the beam sources are mounted on the rotatable lid of the scattering chamber, they can pivot about the collision center, thus permitting the measurement of angular distributions by the stationary detector.

The individual components of EVA are more fully described elsewhere.[5,12]

Internal States of the Reactants

In addition to controlling the relative translational energy of the reactants, it is also possible to closely define the internal states of the reactants. For the monatomic ion Ar^+ it is necessary to consider only the contributions from various electronic states. The ions are produced by impact of 120-eV electrons. Under these conditions, less than 1% of the resulting ions are in high-energy metastable states.[13] The remainder are in

the ^2P state and should be distributed statistically in a 2:1 ratio between the $J=\frac{3}{2}$ and $J=\frac{1}{2}$ levels. These two levels differ in energy by only 0.18 eV, and we have used the statistical weighting factor of 2:1 to arrive at a weighted average for the heat of formation of Ar^+.

The internal energy of the neutral molecular reactant is determined by the temperature of the gas, which is 328°K under the conditions of the experiment. It is assumed that the gas is in thermal equilibrium, so that the Boltzmann equation is applicable. It can be seen nearly all the D_2 (HD, H_2) molecules are in the ground vibrational state. Moreover, the most probable rotational level is $J=1$, which corresponds to an energy of about 0.01 eV.

Because there is no reliable value for the heat of formation of the product ion, ArD^+ (ArH^+), it is not possible to assign a definite value to the heat of the reaction, ΔH. However, recent data[14] have indicated a "best" value of 3.55 eV for the bond strength of ArH^+ with respect to dissociation into Ar^+ and H. This corresponds to a heat of reaction of -1.20 eV for the $Ar^+ + H_2$ reaction. We can, therefore, conclude that most of our potentially available internal energy will come from the heat of reaction, ΔH.

RESULTS

Typical data, in this case for reactions (3a) and (3b), are shown in Fig. 2 for three different values of the argon-ion beam (lab) energy. Energy spectra, shown at the right section of the figure, were measured at those angles indicated by arrows. These data can be summarized in the form of a velocity vector Newton diagram.[15] (See Fig. 3.) This shows the most probable laboratory velocity of the reactants, $v_{lab}(Ar^+)$ and $v_{lab}(HD)$, the velocity of the center of mass, v(c.m.), and the relative velocity of the reactants, v_{rel}.

Contour lines are constructed to represent the relative intensity of the ionic product as a function of laboratory angle and velocity. These intensities were obtained as follows: The energy spectra at each laboratory angle, Θ are converted to velocity spectra by multiplying each point by the corresponding velocity, v, in accordance with the transformation

$$I_L(E)dE = I_L(v)dv, \tag{5}$$

where I is intensity. The area under each velocity curve is then normalized to the corresponding total intensity at the laboratory angle, Θ, with the intensity at the maximum in the angular distribution being arbitrarily set equal to unity. This yields relative differential cross section, $I_L(v, \Theta, \Phi)$ for a given range of laboratory velocity, dv, and solid angle, $d\Omega = \sin\Theta d\Theta d\Phi$. By plotting the appropriate contours on a velocity vector Newton diagram, there results a plot on intensities as seen by a detector subtending a constant small angle, $d\Omega$, and densitive to velocities between v and $v+dv$. (See Fig. 3.)

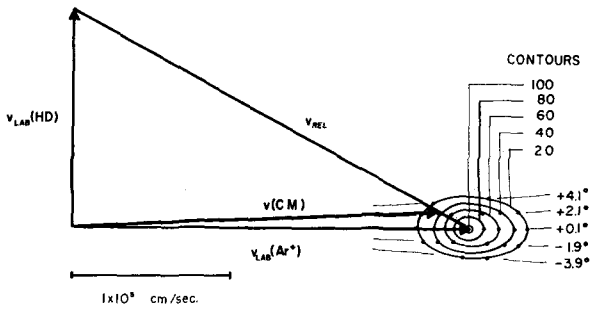

FIG. 3. Newton diagram for the reaction Ar^+ (1.31 eV lab) + HD = ArH^+ + D, constructed from data in Fig. 2(a). Relative intensity of ArH^+ for given lab ordinates $v_{lab}(Ar^+)$, Θ and corresponding c.m. ordinates $u(ArH)^+$ are shown as contours. These intensities are relative to the lab system, i.e., they are intensities as seen by a detector subtending a given solid angle with respect to the lab origin, and sensitive to particles with velocities between $\mathbf{v}$ and $\mathbf{v}+d\mathbf{v}$.

The extraction of information concerning the dynamics of the reaction from such a Newton diagram is complicated by the fact that its velocity space is symmetric only with respect to the laboratory (lab) origin, i.e., the volume elements in the Newton diagram are not constant but vary as v^2. This results in an apparent distortion of the intensity distribution, with undue emphasis being given to regions of higher velocity.

One solution to this problem is to transform the lab cross section, I_L, to similar cross sections, $I_{c.m.}(u, \theta, \phi)$, referred to an origin at the center of mass. The transformation relationship is[16]

$$I_{c.m.}(u, \theta, \phi) = (u^2/v^2) I_L(v, \Theta, \Phi). \tag{6}$$

Such a c.m. system is useful because it allows one to check that the product distribution is symmetric about the collision axis (relative velocity vector) and to determine the degree of forward–backward symmetry.

However, since most molecular beam experiments involve beams with velocity and angular spreads in one or both of the beams, there is no unique center of mass. The usual procedure of calculating a most probable center of mass has the disadvantage of obscuring information near the center of mass by creating there a "hole" in the intensity distribution due to the factor (u^2/v^2) approaching zero.

These difficulties may be overcome by using Cartesian velocity space rather than the polar coordinate systems of the lab or c.m. conventions.[17] The probability of finding product in a given volume of velocity space P_C or P_C' is simply related to the intensities in the lab and c.m. system[17]

$$P_C(v_x, v_y, v_z) = P_C'(u_x, u_y, u_z) = I_L/v^2 = I_{c.m.}/u^2. \tag{7}$$

Since the origin of the Cartesian system is arbitrary, it is independent of any assumptions made in calculating the position of the center of mass. Further, the distortion due to the unequal size of volume elements in

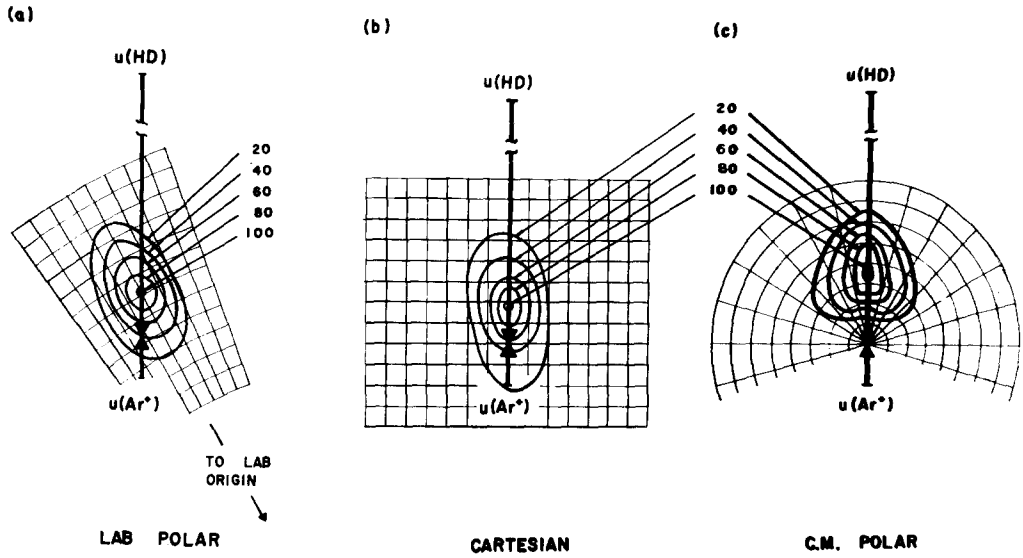

FIG. 4. Modified Newton diagrams, showing the data from Fig. 3 with respect to the relative velocity vector. Arrows represent CM velocities of $Ar^+[\mathbf{u}(Ar^+)]$ and $HD[\mathbf{u}(HD)]$; point of meeting of arrows represents position of the center of mass. (a) ArH^+ intensity, I_L, relative to the lab polar coordinate system, as in Fig. 3; (b) same data, as probabilities, P_C', relative to Cartesian system, i.e., intensities as seen by a detector sensitive to particles in an element $du_x du_y du_z$ of velocity space; (c) same data, as intensities $I_{c.m.}$, relative to c.m. polar system, i.e., intensities as seen by a detector subtending a given solid angle with respect to c.m. origin and sensitive to particles with velocities between $\mathbf{u}$ and $\mathbf{u}+d\mathbf{u}$.

the lab polar system has been removed, so that P_C possesses all the symmetry properties of $I_{c.m.}$ about any chosen center of mass. Tests for axial and forward–backward symmetry can thus be made as well with the Cartesian system as with the c.m. polar system. Finally, because the volume elements are of equal size in the Cartesian system, the "hole" near the assumed center of mass is no longer present. Figure 4 presents for comparison the results of the same experiment in the three different coordinate systems.

From data such as that shown in Fig. 2, Newton diagrams (shown in Fig. 5) were constructed to present the Cartesian probabilities ($P_C=I_L/v^2$) of the ionic products of Reactions (3a) and (3b) at five energies of the incident Ar^+ ion beam. In principle, the distributions should be totally symmetric about the collision axis. The extent of deviation from cylindrical symmetry in Fig. 5 is about what to expect from the spread in beam energies.

Since, for the purposes of this investigation, the position of the maximum of the product ion intensity with respect to the center of mass was of primary importance, another technique was also employed as an alternative to the construction of the complete Newton diagram. The product ion angular distribution was measured to determine the angle of maximum intensity. For this angle the most probable product energy was measured and the corresponding center-of-mass velocity calculated. (To be rigorously correct, the energy spectrum in the lab system should first have been converted to the corresponding lab velocity spectrum by multiplying the intensity at each point by the velocity, v; then, the lab velocity spectrum converted to a Cartesian spectrum by multiplying each point by $1/v^2$. However, the product energy spectra were so sharply peaked that multiplication by the over-all Jacobian factor of $1/v$ shifted the position of the product peak by less than 1%, considerably less than the estimated experimental error.) Such data for Reactions (2), (3a), (3b), and (4) are summarized in Table I.

DISCUSSION

Direct Mechanism vs Long-Lived Intermediate

A good test for the formation of a long-lived intermediate is the shape of the product distribution about the center of mass. If a complex that rotated many times were formed, the product distribution would necessarily be symmetric with respect to the plane passing through the c.m. and perpendicular to the relative velocity vector. As shown in Fig. 5, the product distributions are clearly asymmetric about the c.m., in agreement with our earlier findings[5] for the argon-ion–deuterium reaction. This asymmetry is a clear indication that, even at the lowest energy measured (less than 0.1 eV c.m.), the contribution of any long-lived intermediate is small and that reaction is dominated by a direct mechanism.

The relatively small back-scattered intensity found by Bailey[3] and interpreted as indicating a contribution from a long-lived complex could also represent a rebound process occurring by a direct mechanism. Such an explanation has been put forward[4] to account for

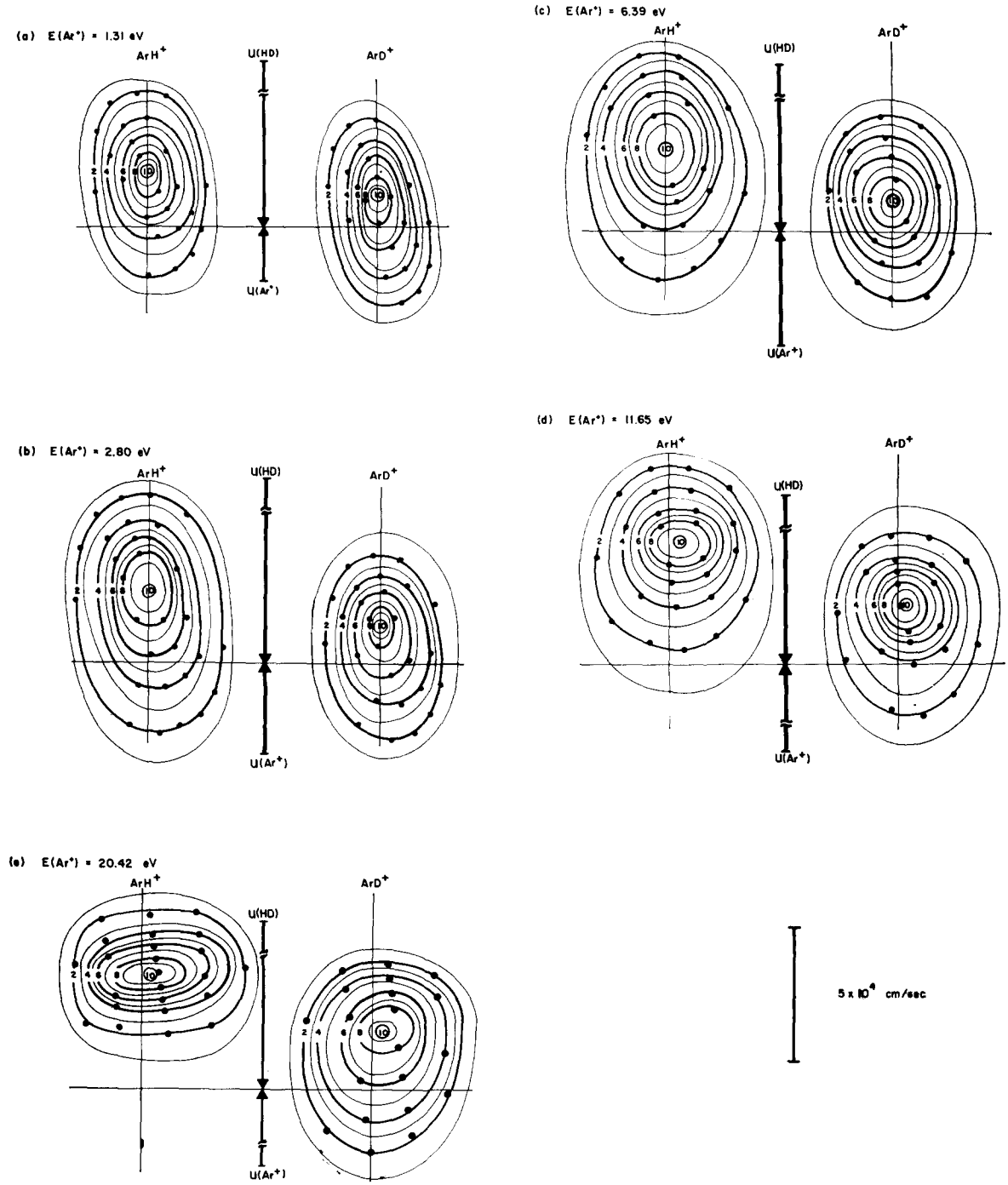

FIG. 5. Product probability diagrams for the reaction of Ar^+ with HD at five lab energies of the Ar^+ beam. ArH^+ and ArD^+ intensities, independently normalized to unity, are shown relative to the Cartesian system, P_C. Experimental points on odd contour lines have been omitted.

the back-scattered peak observed at high energies where the small reaction cross section implies a small range of impact parameters, and a high likelihood of near head-on collisions. While the product distribution is largely forward there is an increasingly significant amount of back-scattered product as the initial energy decreases. Similar observations were made in our earlier work[5] and by Bailey *et al.*[3] The latter interpreted this phenomenon as indicating a contribution from a long-lived complex mechanism. Whether this is actually the case seems doubtful. As will be discussed below, our model of direct reaction qualitatively predicts the observed increase in back scattering at low energies. Hence, these results provide no evidence whatsoever

TABLE I. Data for reactions of the type $X^+ + YZ \rightarrow XY^+ + Z$.

Most probable lab energy of X^+ (eV)	Most probable lab energy of XY^+ (eV)	Lab angle of maximum product intensity (degrees)	Translational exoergicity Q (eV)
A. $Ar^+ + H_2 \rightarrow ArH^+ + H$			
1.04	1.08	0.0	+0.110
1.59	1.63	0.0	+0.108
1.93	1.96	0.0	+0.090
2.35	2.35	0.2	+0.028
2.94	2.94	0.2	+0.030
3.16	3.14	0.2	+0.002
3.86	3.83	0.2	−0.010
3.89	3.82	0.0	−0.040
4.23	4.20	0.2	−0.008
4.41	4.35	0.2	−0.046
4.65	4.58	0.2	−0.058
4.80	4.72	0.2	−0.069
4.82	4.72	0.2	−0.092
5.35	5.22	0.2	−0.123
5.88	5.78	0.2	−0.091
5.92	5.83	0.3	−0.088
7.13	7.00	0.4	−0.141
7.70	7.55	0.2	−0.145
9.05	8.90	0.3	−0.154
11.02	10.75	0.3	−0.282
11.25	11.04	0.3	−0.218
12.50	12.25	0.2	−0.250
15.64	15.40	0.2	−0.232
16.07	15.85	0.3	−0.218
17.77	17.46	0.2	−0.308
17.81	17.33	0.2	−0.486
19.81	19.33	0.2	−0.489
20.03	19.63	0.1	−0.389
22.69	22.28	0.2	−0.411
24.04	23.60	0.1	−0.425
24.77	24.33	0.0	−0.400
27.08	26.60	0.0	−0.439
30.15	29.70	0.1	−0.419
30.69	30.05	0.1	−0.633
34.41	33.72	0.1	−0.682
40.63	39.93	0.1	−0.679
43.38	42.68	0.1	−0.670
57.86	56.75	0.1	−1.098
71.15	69.50	0.1	−1.656

Most probable lab energy of X^+ (eV)	Most probable lab energy of XY^+ (eV)	Lab angle of maximum product intensity (degrees)	Translational exoergicity Q (eV)
B. $Ar^+ + D_2 \rightarrow ArD^+ + D$			
0.60	0.65	0.2	+0.125
0.61	0.63	0.3	+0.060
0.65	0.69	0.3	+0.100
0.71	0.79	0.6	+0.183
1.68	1.68	0.2	+0.039
1.93	1.94	0.3	+0.052
2.23	2.24	0.2	+0.060
2.29	2.25	0.2	−0.011
2.71	2.65	0.0	−0.022
3.38	3.26	0.0	−0.089
3.89	3.78	0.3	−0.094
4.38	4.29	0.3	−0.065
4.46	4.36	0.3	−0.078
5.24	5.08	0.5	−0.158
7.17	6.99	0.0	−0.132
8.05	7.80	0.3	−0.237
14.31	14.02	0.0	−0.204
15.00	14.55	0.3	−0.432
17.65	17.15	0.3	−0.473
21.07	20.40	0.3	−0.653
21.24	20.55	0.3	−0.675
24.65	23.90	0.2	−0.713
26.43	25.50	0.0	−0.879
27.75	26.77	0.0	−0.929
31.10	29.88	0.0	−1.180
31.44	30.35	0.1	−1.052
33.35	32.15	0.0	−1.147
34.56	33.15	0.1	−1.393
36.38	35.10	0.1	−1.241
36.45	34.90	0.0	−1.516
C. $Ar^+ + HD \rightarrow ArH^+ + D$			
1.61	1.68	0.2	+0.114
1.63	1.73	0.2	+0.166
1.98	2.06	0.2	+0.128
2.17	2.24	0.3	+0.106
2.25	2.32	0.3	+0.106
2.57	2.58	0.2	+0.025

TABLE I (*Continued*)

Most probable lab energy of X^+ (eV)	Most probable lab energy of XY^+ (eV)	Lab angle of maximum product intensity (degrees)	Translational exoergicity Q (eV)
2.79	2.85	0.4	+0.085
3.37	3.41	0.5	+0.052
3.94	3.97	0.2	+0.053
4.40	4.40	0.0	+0.028
5.42	5.35	0.2	−0.066
6.42	6.33	0.0	−0.072
6.71	6.63	0.0	−0.060
8.48	8.40	0.0	−0.056
10.20	10.08	0.0	−0.097
12.90	12.75	0.0	−0.125
16.67	16.40	0.0	−0.250
20.18	19.90	0.0	−0.254
25.13	24.72	0.0	−0.387
30.78	30.15	0.0	−0.613
D. $Ar^+ + HD \rightarrow ArD^+ + H$			
1.61	1.62	0.5	+0.080
1.98	1.94	0.3	+0.007
2.17	2.12	0.5	−0.020
2.23	2.18	0.5	−0.020
2.25	2.21	0.3	+0.011
2.57	2.52	0.2	+0.009
2.79	2.71	0.3	−0.042
3.37	3.27	0.4	−0.073
3.94	3.83	0.4	−0.081
4.40	4.20	0.4	−0.189
5.42	5.13	0.2	−0.259
6.42	6.23	0.5	−0.173
6.71	6.42	0.0	−0.232
8.48	8.20	0.2	−0.237
10.20	9.80	0.0	−0.335
12.90	12.48	0.2	−0.372
16.67	15.80	0.0	−0.810
20.18	19.16	0.0	−0.961
25.13	23.95	0.0	−1.123
30.78	29.50	0.0	−1.211

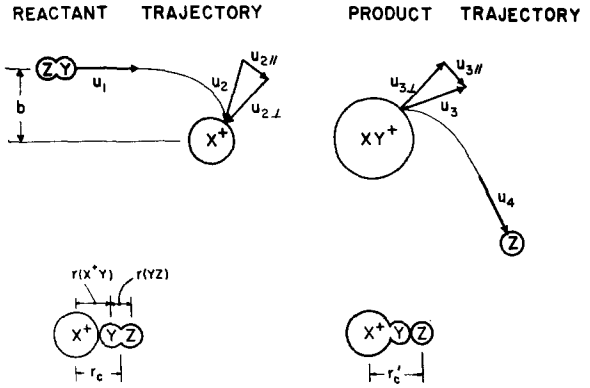

FIG. 6. Schematic representation of reaction between X^+ and YZ. Upper portion shows how a molecule YZ approaching X^+ with initial relative velocity u_1 and initial impact parameter b smaller than the classical Langevin[24] value, $b_{max}=(2\alpha e^2/T_1)^{0.25}$, is captured. YZ is accelerated towards the ion by the ion-induced dipole force so that the relative velocity has increased to u_2 by the time the critical reaction radius, r_c, is reached. The relative velocity at this point, u_2, may be resolved into components parallel ($u_{2||}$) and perpendicular ($u_{2\perp}$) to the reaction surfaces. Transfer of Y to X occurs, leaving products separated by distance r_c', and with a relative velocity u_3. As they recede from one another, they are decelerated so that at infinite separation their relative velocity is u_4. The lower portion is a schematic representation of the reactants just prior to transfer, and products just after transfer, showing the assumptions made in the calculation of the potential energy terms, P and P'.

for the formation of any persistent intermediate complexes at any energy.

The fact that no persistent complexes appear to be involved is not surprising. RRK theory[18] suggests that the magnitude of the lifetime of such a complex with respect to unimolecular decomposition is

$$\tau \cong 10^{-13}[(E-E^*)/E]^{1-s} \text{ sec.} \quad (8)$$

Here E is the total energy of the complex, E^* is its stability with respect to decomposition, and s is the number of normal vibrational modes. Since the Reaction (2) is exothermic by about 1.2 eV, $E>E^*+1.2$ eV. Therefore, even if s is the maximum possible value (i.e., 3), E^* would have to be several electron volts for the lifetime of the complex to be equal to one rotational period (10^{-12} sec). Such a high value seems quite unlikely on the basis of bonding theory.

The original basis for the supposed complex formation at low energies was an interpretation[19] of observed isotope effects on reaction cross sections in terms of unimolecular decomposition of $ArHD^+$. Both Light[20] and Suplinskas[21] have now shown that direct mechanisms such as proposed here and in our earlier work,[5] would predict isotope effects similar to those actually observed.

TABLE II. Glossary of terms.

u_j	Relative velocity of particles in jth stage of reaction
u_{ji}	c.m. velocity of particle i in jth stage of reaction
$j=1$	Reactants at infinite separation
$=2$	Reactants at distance of closest approach, r_c
$=3$	Products at distance of closest approach, r_c'
$=4$	Products at infinite separation
μ	Reduced mass of reactants, (X)(Y+Z)/(X+Y+Z)
b	Initial impact parameter
T_j	Total c.m. kinetic energy in jth stage of reaction
T_{ji}	c.m. kinetic energy of particle i in jth stage of reaction
α_i	Polarizability of particle i
e	Electronic charge
P	Potential energy converted into kinetic energy in bringing reactants from infinite separation of distance of closest approach, r_c
Q	Translational exoergicity, T_4-T_1

Model for Direct Transfer Reactions

We treat the generalized transfer reaction

$$X+YZ\rightarrow XY+Z \tag{9}$$

as it occurs in the center-of-mass coordinate system. In the first stage of reaction (reactants at infinite separation), the reactants approach with an initial relative velocity u_1 and impact parameter b (see Fig. 6). The relative kinetic energy is

$$T_1=1/2\mu u_1^2, \tag{10}$$

where μ is the reduced mass of the reactants (see Table II). As they approach one another, the attractive potential (ion-induced dipole potential in the case of ion–molecule reactions) accelerates them so that their kinetic energy at the distance of closest approach r_c (stage 2, just prior to transfer) is

$$T_2=T_1+P, \tag{11}$$

where P is the kinetic energy gained between ∞ and r_c.

The relative velocity, u_2, at distance r_c may be resolved into components parallel and perpendicular to the reaction surface, $u_{2||}$ and $u_{2\perp}$, respectively (see Fig. 6). This partition is determined by the impact parameter b and the initial relative velocity u_1 through conservation of angular momentum:

$$\mu b u_1=\mu r_c u_{2||}. \tag{12}$$

Defining total relative kinetic energies corresponding to the parallel and perpendicular velocity components, $T_{2||}=1/2\mu u_{2||}^2$ and $Y_{2\perp}=1/2\mu u_{2\perp}^2$, Eq. (12) implies

$$T_{2||}=(b/r_c)^2T_1 \tag{13}$$

and

$$T_{2\perp}=T_2-T_{2||}=P+[1-(b/r_c)^2]T_1. \tag{14}$$

Transfer of Y to X now occurs. In stage 3 the products at a distance of closest approach, r_c', start to separate. Their initial relative kinetic energy T_3 is

$$T_3=1/2\mu' u_3^2, \tag{15}$$

where μ' is the reduced mass of the products.

We now make the following assumptions to govern the partition of u_3 into components parallel ($u_{3||}$) and perpendicular ($u_{3\perp}$) to the reaction surface:

Assumption A: We assume that the velocity component of the freed particle, Z, parallel to the reaction surface, $u_{3||Z}$, is the same as it was when Z was combined in the reactant, i.e.,

$$u_{2||YZ}=u_{3||Z}. \tag{16}$$

The corresponding kinetic energies of YZ just before transfer and Z just after transfer are then related by Eq. (16) as

$$T_{3||Z}=[(Z)/(Y+Z)]T_{2||YZ}. \tag{17}$$

Assumption B: We assume that the kinetic energy of the products corresponding to the perpendicular component of their relative velocity $T_{3\perp}$, is related to the similar quantity, $T_{2\perp}$, by some multiple, λ[22]:

$$T_{3\perp}=\lambda T_{2\perp}=\lambda P+\lambda[1-(b/r_c)^2]T_1. \tag{18}$$

The products, XY and Z, are now decelerated by the attractive potential between them, so that in the fourth stage of reaction (products at infinite separation) their kinetic energy is

$$T_4=T_3-P'=T_{3||}+T_{3\perp}-P', \tag{19}$$

where P' is the gain in potential energy in moving from r_c' to infinity.

We are now able to calculate T_4 as a function of T_1. From the conservation of momentum conditions,

$$T_{3||}=[(X+Y+Z)/(X+Y)]T_{3||Z}, \tag{20a}$$

$$T_{2||}=[(X+Y+Z)/X]T_{2||YZ}, \tag{20b}$$

and the preceding equations it readily follows that

$$T_4=(\lambda P-P')+\{(b/r_c)^2\{[(X)(Z)/(X+Y)(Y+Z)]-\lambda\}+\lambda\}T_1. \tag{21}$$

Correspondingly the velocity u_{4XY} (in terms of which the data in this work is presented) is given by

$$u_{4XY}=[2ZT_4/(X+Y)(X+Y+Z)]^{1/2}. \tag{22}$$

A quantity of special interest is the translational exoergicity, Q, the net difference between the final and initial kinetic energies,

$$Q=T_4-T_1. \tag{23}$$

This may be conveniently expressed in terms of the translational exoergicity at zero initial energy, Q_0,

$$Q=Q_0+BT_1, \tag{24}$$

where, by the model

$$Q_0=\lambda P-P' \tag{25}$$

and

$$B=\lambda-1+(b/r_c)^2\{[(X)(Z)/(X+Y)(Y+Z)]-\lambda\}. \tag{26}$$

Spectator-Stripping Model

In spectator stripping[1] all intermolecular forces are ignored, so that $P=P'=0$. Moreover, the resulting straight-line trajectories dictate that $r_c=b$. Therefore,

$$T_4=[(X)(Z)/(X+Y)(Y+Z)]T_1 \tag{27}$$

and

$$Q=-\{1-[(X)(Z)/(X+Y)(Y+Z)]\}T_1. \tag{28}$$

Polarization-Stripping Model

In this model the acceleration due to attractive interactions is taken into account.[5] The spectator-stripping model is retained to the extent that the magnitude of the c.m. velocity of particle Z is unchanged by the transfer

$$|u_{3Z}|=|u_{2YZ}|. \tag{29}$$

It can readily be shown that this assumption requires that λ in Eq. (18) be given by the expression

$$\lambda=(X)(Z)/(X+Y)(Y+Z). \tag{30}$$

Substitution of this result in the equations for T_4 and Q yields

$$T_4=\frac{(X)(Z)}{(X+Y)(Y+Z)}P-P'+\frac{(X)(Z)}{(X+Y)(Y+Z)}T_1, \tag{31}$$

and

$$Q=\frac{(X)(Z)}{(X+Y)(Y+Z)}P-P'-\left[1-\frac{(X)(Z)}{(X+Y)(Y+Z)}\right]T_1. \tag{32}$$

Note that this is not strictly a stripping model in that although the magnitude of the velocity of the freed particle is unchanged by the transfer, its direction may be modified.

The requirement of Eq. (16) that the component of velocity of particle Z parallel to the reaction surface remain constant is physically reasonable for any model of transfer reactions because the forces involved are presumed to be radial rather than tangential in nature. It is more difficult to conceive of a situation in which the perpendicular component remains unchanged in magnitude. This would happen if the bond in YZ was so weakened just prior to transfer of Y to X that the particles were essentially traveling independently. Z could then be elastically scattered off XY, its speed remaining unchanged. Note, however, that Y and Z must remain strongly coupled during the preceding acceleration phase; otherwise (unless they were identical) they would not have a common velocity.

Polarization–Reflection Model

The physical picture underlying this model is as follows: YZ collides with X, and the kinetic energy corresponding to the perpendicular component of their relative velocity is transformed to potential energy. At this point, Y is transferred to X, and Z is released. The kinetic energy gained as XY and Z recoil from each other, $T_{3\perp}$, depends on the compression of Z against XY. As such, we assume it to be a constant fraction, λ, of the energy that went into the compression, $T_{2\perp}$, regardless of the isotopic mass of Z. This contrasts with the polarization-stripping model where the velocity of Z remains the same as that of YZ, and where its energy would therefore depend on its mass. The difference, of course, is that in the latter case Y and Z are uncoupled so that they make the final collision independently, whereas in the present model YZ remains as a unit until the products start to separate.

If Z and XY carry off half the kinetic energy corresponding to motion perpendicular to the reaction surface, $\lambda=\frac{1}{2}$, and we call the reflection "quasielastic," or simply "elastic." If $\lambda>\frac{1}{2}$, the term "superelastic," and if $\lambda<\frac{1}{2}$, the term "subelastic" may be used. The former situation obtains if there is a strong short-range repulsion between XY and Z, the latter if this repulsion is relatively weak. (This terminology is obviously nonrigorous and should not be too literally interpreted. Its usefulness is most readily apparent on considering the common type of system X+YZ→XY+Z, where X is much more massive than YZ. The freed Z can then be considered as scattering elastically or otherwise off the newly formed XY).

Comparison of the Models

The differences between these models are apparent primarily at lower energies. At higher initial energies T_1, the attractive potential terms P and P' become relatively negligible. This means that the final kinetic energy, T_4, predicted by the polarization-stripping model [Eq. (34)], approaches that of spectator stripping [Eq. (30)]. The same is true for the polarization-reflection model if Y=Z. If Y≠Z, T_4 will depend upon (b/r_c). Over a certain higher energy range (where the reaction cross section approximates the geometrical cross section), b is similar to r_c, and this model would then also make the same prediction for T_4 as does spectator stripping.

The final c.m. velocity of the product, u_{4XY}, is particularly sensitive to the model at low energies. In spectator stripping it will be a constant fraction of the reagent velocity, u_{1X}, and will thus tend to zero at zero collision energy. The other models, though tending toward spectator stripping at high energies, will generally predict rapid variations of u_{4XY}/u_{1X} at low ener-

TABLE III. Model predictions for translational exoergicity, $Q=Q_0+BT_1$.

Model	If $X\gg Y$ and $Y=Z$.		If $X\gg Y$ and $Y=2Z$.		If $X\gg Y$ and $Y=\frac{1}{2}Z$.	
	Q_0	B	Q_0	B	Q_0	B
I. Spectator stripping	0	$-\frac{1}{2}$	0	$-\frac{2}{3}$	0	$-\frac{1}{3}$
II. Polarization stripping	$\frac{1}{2}P-P'$	$-\frac{1}{2}$	$\frac{1}{3}P-P'$	$-\frac{2}{3}$	$\frac{2}{3}P-P'$	$-\frac{2}{3}$
III. Polarization–elastic reflection	$\frac{1}{2}P-P'$	$\approx-\frac{1}{2}$	$\frac{1}{2}P-P'$	$\approx-\frac{1}{6}(b/r_c)^2-\frac{1}{2}$ ($\approx-\frac{2}{3}$)[a]	$\frac{1}{2}P-P'$	$\approx\frac{1}{6}(b/r_c)^2-\frac{1}{2}$ ($\approx-\frac{1}{3}$)[a]

[a] Limiting value at higher energies if $b\approx r_c$.

gies and a finite product velocity at zero initial energy ($T_1=0$). (If P' is relatively large, it is also possible that T_4 and u_{4XY} will be negative. This means that the attraction between the products is so strong that they cannot separate. This may result in the reactants reforming, or the reaction going by a different mechanism including possible intermediate persistent-complex formation.)

Experimental data may also be used to evaluate the translational exoergicity, Q. The behavior of this function for each of the several models is shown in Table III. Of particular interest is the translational exoergicity at zero initial energy, Q_0. This is zero for spectator stripping and finite for the other models. It is seen that if X≫Y and Y=Z, as was the case in our earlier work[5] on Reactions (1) and (2), Q_0 is the same for both polarization stripping and polarization reflection. These mechanisms are, however, distinguishable on this basis if Y≠Z, as is true in the present study of Reactions (3a) and (3b).

In the above discussions "high" and "low" energies are taken as relative to the attractive potentials, P and P'. In the case of ion–molecule reactions the latter are of the order of 1 eV. Thus these mechanisms are best differentiated at low c.m. energies of only a few tenths of an electron volt. Indeed, these very simple models should not be expected to hold at very high energies (>10 eV c.m.). At such energies the required energy disposal in internal modes may lead to product dissociation. Reactions leading to formation of XY in a bound state will thus favor disposition of extra energy in translation and consequently lead to higher Q values. Such effects have been identified by Henglein[2] and Bailey[3] and are not accommodated in the framework of these models, which are primarily intended for the low and medium energy range.

Angular Distributions

The angular distributions of the products as predicted by these models are not quantitatively developed here. Some remarks on their qualitative character are nevertheless appropriate.

Spectator stripping demands, by definition, that the velocity vector of the freed particle be unchanged with respect to the reactant in which it was originally contained. If the direction of X is taken as "forward," then all XY will appear at 0°, and all Z at 180° in the center-of-mass system.

The angular distributions of polarization stripping and polarization reflection will most closely resemble that of spectator stripping at medium to high energies, i.e., when the initial energy, T_1, is fairly large compared to the potentials P and P'. The attractive forces will then cause no appreciable deflection of either reactants or products. Furthermore, in this energy range the cross section often tends to be "geometrical" in the sense that the most common type of reactive collisions occur at a grazing incidence so that $b=r_c$. The velocity component normal to the reaction surface, $u_{2\perp}$, then tends to be small. Thus, there is frequently little deflection due to the repulsive as well as the attractive potential.

At very high energies, however, the reaction cross section becomes very small due to the difficulty of conserving both momentum and energy in the reaction. Reaction may then occur more readily when the collision is more nearly "head on," i.e., $b<r_c$. The normal velocity component $u_{2\perp}$ may now be relatively large. The repulsive potential can then cause wide deviation from spectator stripping.[23] Backward "rebound" as well as forward scattering will result. Such effects have been observed and analyzed by Bailey,[3] Mahan,[4] and collaborators.

At low energies both polarization models will also show considerable deviation from spectator stripping. However, this is then due to the attractive potentials, P and P', which are now comparable to or larger than the initial energy, T_1. For reactions without threshold, cross sections become very large compared to "geometrical" dimensions because of the "pulling-in" effect of the attractive force. Thus for most reactive collisions, b is much greater than r_c. The reactants then follow trajectories appreciably curved, or may even spiral into one another. Likewise, the products will also follow curved trajectories, thus causing the product directions to deviate significantly from those of the reactants. As the initial energy, T_1, decreases to become comparable to and then smaller than the polarization potentials, there should be increasing deviations from spectator

stripping. When the maximum impact parameter becomes sufficiently large so that spiraling can go through 180°, a backward peak will be observed. "Rebound" scattering can thus be expected to occur at low as well as at relatively high energies, although the reasons for its occurrence are then quite different. (It is worth noting that this increasing backward component may give the appearance of a partial approach to forward–backward symmetry as the energy is decreased in the low range. This, in turn, may readily be mistaken as evidence for some low-energy contribution by a mechanism involving a persistent intermediate complex.)

Ion–Molecule Reactions

To apply this model to ion–molecule reactions in a quantitative way, four working assumptions were made: (1) The ion-induced dipole depends on r^{-4} over all distances of separation. (This approximation is strictly correct only for r approaching infinity.) (2) The X^+–YZ complex is linear at the moment when Y is transferred. (This assumption also implies that the parallel polarizability of YZ should be used.) (3) The charge is localized at the center of X^+ throughout the course of the reaction. (4) The YZ bond distance remains unchanged until reaction occurs.

The approximations permit the evaluation of the potential energy terms P and P' (see Fig. 6):

$$P=\alpha_{YZ}e^2/2r_c^4, \tag{33}$$

and

$$P'=\alpha_Z e^2/2r_c'^4, \tag{34}$$

where α_i is the polarizability of species i, and e is the electronic charge.

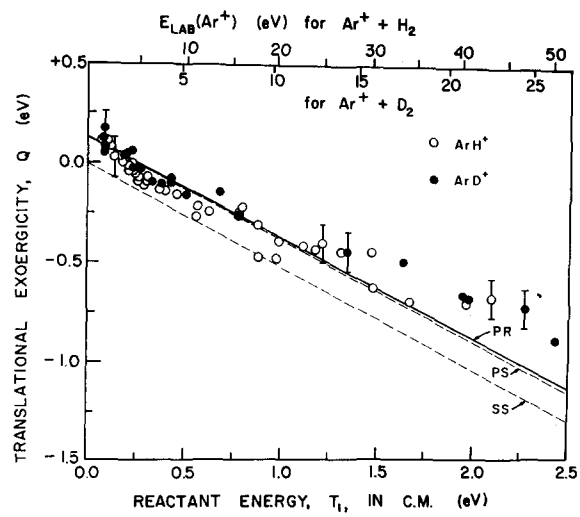

FIG. 7. Translational exoergicity Q vs initial relative energy T_1 for reactions of Ar^+ with H_2 and D_2 (data taken from Tables I.A and I.B). Estimated limit of experimental uncertainty are indicated by error bars for several of the points. The line SS shows Q vs T_1 dependence predicted by spectator-stripping model; PS is prediction of polarization-stripping model; PR is prediction of polarization–reflection model. The two variations of the polarization models predict the same dependence for ArH^+ and ArD^+, within the width of the line.

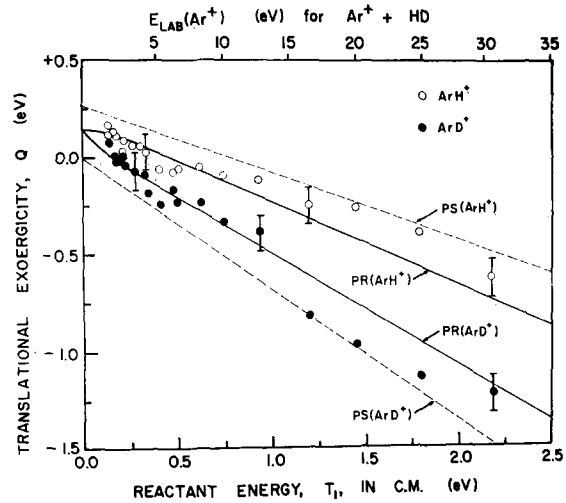

FIG. 8. Q vs T_1 for the reaction of Ar^+ with HD (data from Tables I.C and I.D). PS(ArH^+) and PS(ArD^+) represent the predictions of the polarization-stripping model when the ionic product is ArH^+ and ArD^+, respectively. PR(ArH^+) and PR(ArD^+) show the corresponding predictions of the polarization-elastic-reflection model.

The model is normalized to the data at the lowest energy by adjusting the parameters r_c and r_c'. These are related as shown in Fig. 6. In the case that Y and Z are identical or isotopic,

$$r_c=r(X^+Y)+\tfrac{1}{2}r(YZ), \tag{35}$$

and

$$r_c'=r(X^+Y)+r(YZ). \tag{36}$$

In those expressions for T_4 and Q involving the impact parameter, the mean value $\langle b\rangle$ was used, where

$$\langle b\rangle=b_{\max}/(2)^{1/2}. \tag{37}$$

The maximum impact parameter, $b_{\max}$, was calculated from the Langevin expression for the reaction cross section, σ,[24]

$$\sigma(T_1)=\pi b_{\max}^2=2\pi(\alpha e^2/2T_1)^{1/2}. \tag{38}$$

The model is then tested by determining whether the reaction distance is reasonable and by using the same parameters to predict results at higher energies.

Comparison with Data

For the Ar^+ reactions, we take $\alpha_{H_2}=0.93\times10^{-24}$ cm^3 [25] and 0.74 Å as the H–H bond distance.[26] T_4 is calculated from the c.m. velocity of the product ion at the peak of its intensity in the Newton diagram (Cartesian coordinates), or from the peak in its energy distribution at the lab angle of maximum intensity as explained previously.

$$Ar^+ + D_2 = ArD^+ + D; \qquad Ar^+ + H_2 = ArH^+ + H$$

Data from Tables I.A and I.B for these reactions are plotted as Q vs T_1 in Fig. 7. Extrapolation to zero initial relative energy yields an intercept $Q_0=+0.15\pm0.05$ eV.

This is in obvious disagreement with the spectator-stripping model, which predicts a zero intercept. As shown in Table III, either polarization model predicts an intercept of approximately $Q_0=(\frac{1}{2})P-P'$ for both of these reactions. The observed intercept corresponds to a closest Ar^+–H (Ar^+–D) distance of 1.32±0.10 Å.[27] This agrees well with the known bond distance of 1.27 Å for the isoelectronic molecule HCl. The predictions of the models as to the value of Q at all energies, calculated using the same value $r(X^+Y)=1.32$ Å, are shown in Fig. 7 for the polarization-stripping (PS) model, the polarization–reflection (PR) model, and the spectator-stripping (SS) model. As expected from the results in Table III, either of the polarization models can account for the low-energy results observed for both isotopic systems within experimental error. The apparent positive deviation at higher energies is in line with the factors discussed above.

$$Ar^+ + HD = ArH^+(ArD^+) + D(H)$$

Data from Tables I.C and I.D for these reactions are shown in Fig. 8 in the form Q vs T_1. Also shown are the predictions of both variations of the polarization model, calculated using the Ar^+–H(Ar^+–D) bond distance determined from Fig. 7. As previously discussed (see Table III), the two variations predict significantly different results when $(Y)\neq(Z)$. Due to the splitting of the product ion intensity between the two reaction channels, there is somewhat greater scatter of the experimental points than in Fig. 7. However, the data show much better agreement with the prediction of the polarization–reflection model than with that of the polarization-stripping model, particularly in the critical low-energy region. This is especially evident in the manner in which the points for ArH^+ and ArD^+ seem to be converging toward a common intercept.

SUMMARY AND CONCLUSIONS

Data have been presented on the detailed collision dynamics of a simple ion molecule reaction—that of molecular hydrogen with argon ion to form atomic hydrogen and argon hydride ions. Both velocity and angular distributions of the ionic product were determined as a function of the initial kinetic energy and isotopic variation. As in our previous work we find the reaction to be dominated by a direct mechanism even at c.m. energies as low as 0.1 eV. There is no evidence for participation by a persistent intermediate.

The results are in agreement with our earlier model. This took account of mutual acceleration and deflection of the reactants prior to actual atom transfer, due to the usual long-range attractive potential (ion-induced dipole in the present case); and also a corresponding deceleration of the products on separation. The present data allow us to distinguish between meaningfully different variations of this basic model. In the first, "polarization stripping," the speed of the particle being freed (atomic hydrogen) remains essentially unchanged regardless of its isotopic mass, during the actual transfer. (However the acceleration prior to transfer and the deceleration thereafter will cause a net change in velocity over the whole process.) The mechanism is essentially spectator stripping occurring in the field of the long-range attractive potentials. It implies that either the hydrogen molecule approaches the ion so that the trajectory is tangential at the radius where transfer occurs, or that the hydrogen atoms have in effect become uncoupled just prior to transfer (but not during most of the acceleration phase), so that at the moment of transfer they are essentially moving independently. Both these conditions are perhaps somewhat unrealistic.

In the second variation of the model, "polarization reflection," the reactants, having been mutually accelerated, approach the transfer radius at some angle determined by the initial energy and impact parameter. The component of velocity of the atom being freed which is parallel to the reaction surface is considered to remain unchanged during the transfer. The radial component of velocity may, however, change as the newly freed hydrogen atom recoils away from the newly formed argon hydride ion.

The predictions of both models as to product velocities can be very similar for the systems $Ar^+ + H_2$ and $Ar^+ + D_2$. The reactions between Ar^+ and HD, however, do permit a choice. In the low-energy limit it is found that the kinetic energies of the freed H or D atoms, rather than their velocities, are similar. This means that the polarization-reflection mechanism provides a better representation of the actual process.[28] For this particular reaction it is further found that the velocity of recoil of the freed atom is approximately the same as if a hydrogen atom having the same terminal velocity as the incident hydrogen molecule were elastically scattered off ArH^+. (While the polarization-reflection model should be generally applicable to direct reactions, whether such "elastic reflection" obtains will depend on the process in question. The magnitude of recoil of the product obviously depends on the relative repulsive potentials between the newly-formed products. "Superelastic" and "subelastic" are natural variants of the model.)

No quantitative evaluation of the predictions of either polarization stripping or polarization reflection with respect to angular distribution was made.[29] Qualitatively it is obvious that at initial kinetic energies comparable to the attractive potential the distribution should be strongly forward peaked. At high energies the decreasing cross section and correspondingly greater likelihood of head-on collisions will cause an increasing fraction of backward scattering. At very low energies, where cross sections and impact parameters may be large compared to molecular dimensions, the curved

trajectories of both reactants and products will lead to an appreciable fraction of backward scattering. The data are in accord with these expectations.

ACKNOWLEDGMENTS

This work was made possible by support from the National Aeronautics and Space Administration and the U. S. Atomic Energy Commission. Critical discussions with Dr. John Tully and Mr. James Kerstetter were of great value to the authors.

* Present address: Department of Chemistry, University of Kansas, Lawrence, Kansas 66044.

† Visiting Professor on leave from Institute of Physical Chemistry, Czechoslovak Academy of Science, Prague.

‡ Present address: Sterling Chemistry Laboratory, Yale University, New Haven, Conn. 06520.

[1] A. Henglein, K. Lacmann, and G. Jacobs, Ber. Bunsenges. Physik. Chem. **69**, 279 (1965).

[2] A. Henglein, K. Lacmann, and B. Knoll, J. Chem. Phys. **43**, 1048 (1965).

[3] L. D. Doverspike, R. L. Champion, and T. L. Bailey, J. Chem. Phys. **45**, 4385 (1966).

[4] W R. Bentry, E. A. Gislason, Y.-t. Lee, N. H. Mahan, and C.-w. Tsao, Discussions Faraday Soc. **44**, 137 (1967). W. R. Gentry, E. A. Gislason, B. H. Mahan, and C.-w. Tsao, J. Chem. Phys. **49**, 3058 (1968).

[5] (a) Z. Herman, J. Kerstetter, T. Rose, and R. Wolfgang, J. Chem. Phys. **46**, 2844 (1967); (b) Discussions Faraday Soc. **44**, 123 (1967).

[6] R. D. Fink and J. S. King, J. Chem. Phys. **47**, 1857 (1967).

[7] A. Ding, K. Lacmann, and A. Henglein, Ber. Bunsenges. Physik. Chem. **71**, 596 (1967).

[8] P. Hierl, Z. Herman, J. Kerstetter, and R. Wolfgang, J. Chem. Phys. **48**, 4319 (1968).

[9] When first proposed (Ref. 5) this model was called "modified stripping." It is thought that the term "polarization stripping" is a more accurate description.

[10] It is assumed that the interacting particles have a corresponding Maxwell–Boltzmann distribution in the collision zone [see Ref. 5(b) Footnote 11]. However, Bernstein and co-workers[11] have recently suggested that there may be a deviation from Maxwell–Boltzmann distribution due to deflection of the slower molecules out of the beam. If such a nonMaxwellian distribution does exist in our apparatus it should not, however, make any significant difference in our results or conclusions.

[11] K. T. Gillen, C. Riley, and R. B. Bernstein, J. Chem. Phys. **50**, 4019 (1969).

[12] Z. Herman, J. D. Kerstetter, T. L. Rose, and R. Wolfgang, Rev. Sci. Instr. **40**, 538 (1969).

[13] H. D. Hagstrum, Phys. Rev. **104**, 309 (1956).

[14] J. D. Kerstetter, "Crossed-Beam Studies of the Energy Dependence of Some Simple Ion–Molecule Reactions," Ph.D. dissertation, Yale University, 1969.

[15] D. R. Herschbach, Advan. Chem. Phys. **10**, 332 (1966).

[16] Most published results to date have used the incorrect factor $(u^2/v^2)\cos\delta$,where δ is the angle between u and v. The correct transformation has been given in Ref. 5, Footnote 14, and by W. Miller, S. A. Saffron, and D. R. Herschbach, Discussions Faraday Soc. **44**, 108 (1967).

[17] R. Wolfgang and R. J. Cross, Jr., J. Phys. Chem. **73**, 743 (1969). It should be noted that the Jacobians (u^2/v^2) and $(1/v^2)$ are exact only for a detector infinitesimal in size. They are, however, reasonable approximations provided that the angular acceptance of the detector is small compared to the width of angular distribution. This seems to be the case in the present work, where the angular resolution of the detector is approximately 1° in the horizontal plane and 3° in the vertical.

[18] L. S. Kassel, *Kinetics of Homogeneous Gas Reactions* (Reinhold, New York, 1932), Chap. 5, ACS Monograph.

[19] T. F. Moran and L. Friedman, J. Chem. Phys. **42**, 2391 (1965).

[20] J. C. Light and S. Chan, J. Chem. Phys. **51**, 1008 (1969).

[21] R. Suplinskas and R. Gelb (private communication).

[22] In a variation of the model, Assumption B, i.e., Eq. (18), may be replaced by the condition $T_{3\perp Z}=\lambda T_{2\perp YZ}$. For the systems studied here this variation predicts virtually identical results.

[23] If a "hard-sphere" collision model is assumed, the "rebound" contribution will be overestimated. To make the models more realistic at high energies, it is necessary to remember that the repulsive potential also depends on internuclear separation, and accordingly to use a "soft-sphere" model. This means that the distances of closest approach will at higher energies tend to become smaller than the r_c derived from lower energy data. Reflection of the freed particle will thus in effect occur at smaller radii at higher velocities. Hence, $u_{2\perp}$, will be smaller and forward scattering can still occur even through b may be fairly small.

[24] G. Gioumousis and D. P. Stevenson, J. Chem. Phys. **29**, 294 (1958).

[25] Landolt–Bornstein, *Zahlenwerte und Funktionen* (Springer, Berlin, 1951), Vol. 1, 510. Moelwyn–Hughes, *Physical Chemistry* (Pergamon, London, 1957), p. 373.

[26] Bond distances are taken from Chem. Soc. (London) Spec. Publ. **11**, (1958).

[27] The uncertainty quoted here is based on our estimated uncertainty in the intercept of Q at $T_1=0$. These Q's are based on the most probable velocity in the Cartesian Newton diagrams. In addition, there is, of course, a distribution of Q's corresponding to the distribution of product velocities.

[28] J. Tully (private communication) has considered possible distorting effects due to finite energy resolution of the primary beams and to the finite angular resolution of the detector. It appears that these uncertainties reduce the degree of confidence placed in conclusions which are based on peak values only. Even taking these distorting effects into consideration, however, it is still evident that the polarization–reflection model provides a better representation of the process.

[29] We have just learned that D. T. Chang and J. C. Light [J. Chem. Phys. (to be published)] have calculated angular distributions for the reaction $Ar^+ + D_2 \rightarrow ArD^+ + D$. They used an impulsive reaction model which is essentially identical to what we term the polarization–reflection mechanism. Substantial agreement with experiment as to peak positions and total width of distributions was found. The single adjustable parameter used, namely the Ar^+–D_2 distance, corresponded very closely to that previously deduced[5b] from the velocity distributions. There is some disagreement as to the width of the angular distribution at half-height. This is presumably a result of the oversimplifications inherent in assuming a single reaction radius and configuration.